CZECHOSLOVAK ACADEMY OF SCIENCES

CZECHOSLOVAK JOURNAL OF PHYSICS

REPRINT

VOLUME B 39 1989

CONTROL OF PLASMA POSITION IN THE CASTOR TOKAMAK

M. Valovič

Institute of Plasma Physics, Czechosl. Acad. Sci., Pod vodárenskou věží 4, 182 11 Praha 8, Czechoslovakia

A servo-system for control of plasma position in the CASTOR tokamak is described. The plasma is maintained in the prescribed position with an accuracy of 3 mm.

1. INTRODUCTION

The problem of plasma position is of primary interest in the tokamak design. It is well-known that without precise positioning of the plasma column it is not possible to obtain good discharge parameters and longer pulses. In all modern machines, the plasma position is controlled by more or less expensive servo-systems.

Up to now, the CASTOR tokamak was not equipped with such system. It resulted in large displacements of the plasma column [1]. The present paper describes a simple, low-cost, servo-control system which sufficiently improves the stability of plasma position.

2. POLOIDAL FIELD SYSTEM

The CASTOR tokamak is a small device having major radius $R_0 = 0{\cdot}4$ m. Minor radius, $a = 85$ mm, is defined by a circular aperture limiter. The tokamak operates with toroidal magnetic field $B_T = 1$ T and plasma current $I_p \leqq 25$ kA.

The poloidal magnetic field system consists of copper shell, iron core and active coils. The diagram of the system can be found in [1].

The iron-core transformer has two limbs. The central cylindrical part has radius $R_i = 145$ mm. The core is far from saturation during the whole discharge.

The copper shell has inner radius $b_s = 115$ mm and thickness $d = 10$ mm. Six diagnostic windows in the shell represent 14% of torus length.

The active coils are connected into three quadrupoles. There are two external quadrupole coil systems, placed outside the shell, which generate vertical (3·5 mT/kA) and horizontal (11 mT/kA) magnetic fields. One internal quadrupole coil system for vertical magnetic field (3·8 mT/kA) is placed inside the shell at radius b_s.

In the previously used scenario, both external quadrupole systems were supplied by time-constant currents. The internal quadrupole system was connected in series with the primary transformer winding.

3. SERVO-SYSTEM

The servo-system consists of three parts: detection system, controller and power amplifier. Because of its complexity, a detailed diagram of the complete servo-loop is not presented here. Schematically it is shown in fig. 1. Supporting circuits for

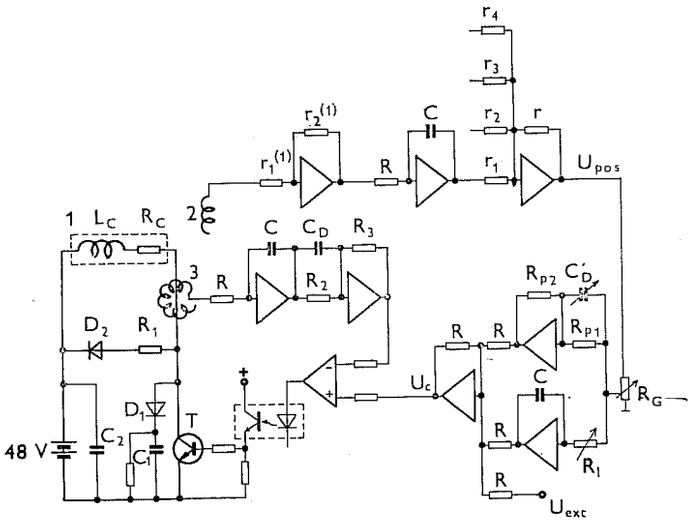

Fig. 1. Schematic diagram of the servo-loop for controlling the radial plasma position. 1 — vertical field coils, 2 — one of the detection coils, 3 — Rogowski coil. Operational amplifiers: TESLA MAC 156 (JFET) for integrators and comparator and TESLA MA 1458 for others. D_1 — TESLA KYW 31/100 (Shottky), D_2 — ČKD D 250, optocoupler: RFT MB 104.

operational amplifiers, elements for balancing the offsets and error signal from toroidal magnetic field are omitted from the drawing.

a) Detection system

The detection scheme used here is a standard one and represents an improved version of that previously used in CASTOR [1]. The outermost magnetic surface of plasma is considered as a perfect toroid with major radius R_p and with circular cross-section of radius a_p. Thus the radial displacement is defined as $\Delta_R = R_p - R_0$. The vertical dispacement Δ_z is the deviation of the plasma torus relative to the centre, of limiter aperture in the direction of major axis (z).

The plasma position is detected by a set of magnetic coils. In one cross-section, there is a complete array of 16 Mirnov coils, uniformly distributed along the poloidal angle ω, and oriented for detecting the poloidal magnetic field $B_\omega(\omega)$. They are placed inside the vacuum chamber in the shadow of the limiter. The coils are mounted on a stainless steel support such that the minor radius of their position is $b = 97$ mm. Each coil consists of 91 turns on cylindrical ceramic form 6 mm in diameter and 30 mm in length. The coil sensitivity is $3{\cdot}7 \times 10^{-3}$ Vs/T. The same support carries one saddle coil having 8 turns and a sensitivity of $14{\cdot}7 \times 10^{-3}$ Vs/T. It measures the vertical magnetic field B_z at this cross-section. All internal coils must be able to withstand the baking of the liner (300 °C) with good vacuum conditions.

Outside the liner, there are two toroidal loops placed in the equatorial plane at minor radius $b' = 110$ mm. The loops are connected in series to detect the toroidally averaged vertical magnetic field:

$$\bar{B}_z = \frac{1}{2\pi R_0} \int_0^{2\pi R_0} B_z(s)\, \mathrm{d}s\,,$$

where s is the length coordinate along the torus. The sensitivity of loops is 0·553 Vs/T.

The signals from the coils are processed by analog circuits based on operational amplifiers. The signal from Mirnov coils are summed with different weights and integrated by Miller integrators ($RC = 12\ \mathrm{k\Omega} \times 0{\cdot}1\ \mu\mathrm{F} = 1{\cdot}2$ ms) providing the plasma current and discrete representation of poloidal moments:

$$\langle B_\omega \cos\omega\rangle = \frac{1}{2\pi}\int_{-\pi}^{\pi} B_\omega(\omega)\cos\omega\,\mathrm{d}\omega\,, \quad \langle B_\omega \sin\omega\rangle = \frac{1}{2\pi}\int_{-\pi}^{\pi} B_\omega(\omega)\sin\omega\,\mathrm{d}\omega\,.$$

The voltages from the saddle and loop coils are amplified and integrated with the same time constant. Finally, by a summation with proper weights, the position signals U_{pos} are obtained. The corresponding weight coefficients are found from Shafranov analytical expression for poloidal magnetic field [2]. For radial and vertical displacements one finds:

$$\begin{aligned} \Delta_R I_p &= -\overline{\langle B_\omega \cos\omega\rangle} + A_2 B_z + A_3 I_p \\ \Delta_z I_p &= -4\pi \langle B_\omega \sin\omega\rangle\, b^2/\mu_0\,, \end{aligned} \tag{1}$$

where $\mu_0 = 4\pi \times 10^{-7}$ H/m and

$$A_1 = 2\pi\left(1 - \frac{a^2}{b'^2}\right)\frac{b^2}{\mu_0 A_0}\,, \qquad A_2 = \pi\left(1 + \frac{a^2}{b^2}\right)\frac{b^2}{\mu_0 A_0}$$

$$A_3 = \tfrac{1}{4}\left(1 + \frac{a^2}{b'^2}\ln\frac{b}{a} + \frac{a^2}{b'^2}\ln\frac{b'}{a} - \frac{a^2}{b'^2} + \ln\frac{b'}{b}\right)\frac{b^2}{A_0 R_0}\,, \quad A_0 = \tfrac{1}{2}\left(1 + \frac{b^2}{b'^2}\right)$$

$$\overline{\langle B_\omega \cos\omega\rangle} = \frac{1}{2\pi R_0}\int_0^{2\pi R_0} \langle B_\omega \cos\omega\rangle\,\mathrm{d}s = \langle B_\omega \cos\omega\rangle + \tfrac{1}{2}(\bar{B}_z - B_z)\,.$$

The last equation is the correction due to the toroidal modulation of vertical fields. In equation (1), the change of a_p during displacement is neglected and we set $a_p = a$.

In electronics, the proportionality constants are given by amplifications $r_2^{(i)}/r_1^{(i)}$ and summation coefficients r/r_i for each particular signal $i = 1, \ldots, 4$ (fig. 1). They must fulfil equations (1) and saturate the operational amplifiers at plasma displacement out of the interest. The following proportionality constants were chosen:

$$\Delta_R = -33{\cdot}3\,\frac{U_{pos,R}}{I_p}\,, \quad \Delta_z = -43{\cdot}3\,\frac{U_{pos,z}}{I_p} \qquad [\mathrm{mm, V, kA}]\,.$$

b) Controller

The position signals are processed by a conventional proportional–plus–integral–plus–derivative controller (see fig. 1). Such controller is characterized by complex

gain which has the form (see e.g. [3]):

$$\hat{G} \equiv \frac{\hat{U}_c}{\hat{U}_{pos}} = G\left(1 + \frac{1}{if\,2\pi T_I} + if\,2\pi T_D\right).$$

Here, $\hat{U}_c$ and $\hat{U}_{pos}$ denote the phasors related to the control voltage U_c and position signal U_{pos} respectively. f is frequency. Real gain $G = \alpha R_{p2}/R_{p1}$, where the coefficient α is set by divider R_G. Time constants are equal to $T_I = R_I C R_{p2}/R_{p1}$ and $T_D = R_{p1} C'_D$. As it was recognized during the experiments, the derivative control is not necessary and therefore in the present work $T_D = 0$.

c) Amplifier

The amplifier works as a unipolar voltage-controlled current source (200 A/V). The similar source is used on the WEGA tokamak [4].

The amplifier which controls radial plasma position is shown in fig. 1. At first, the control voltage is compared with actual current in the winding. Output voltage from comparator controls, via an optical isolation, the main transistor switch T. It consists of one hundred parallel industrial transistors TESLA KDY 76 in the final power stage. In the driver stage, TESLA KD 367 B Darlington transistor is used. The whole switch works with a saturation coefficient of 2 and a current amplification factor of 2×10^6. It is able to switch 2 kA.

The transistor switch is protected by capacitor $C_1 = 24$ mF charged through the fast diode D_1. The capacitor must be able to absorb a great deal of actual current during the switch-on time of the crow-bar diode.

A lead-acid battery bank buffered by capacitor $C_2 = 150$ mF is used as a power supply. The battery gives 1·5 kA stationary current into the load ($R_c = 9$ mΩ).

A maximum slew rate of 1 kA/ms is consistent with the coil inductance $L_c = 36$ μH. A current decay time is chosen to $L_c/R_1 = 1$ ms by a resistance in series with the crow-bar diode. The hysteresis, intrisically given by on/off switching times (10 μs/20 μs), is suppressed by a small capacitance $C_D = 3$ nF in the amplifier ($R_2 = 10$ kΩ, $R_3 = 423$ kΩ) thus adding a small derivative term to the actual current in the coils. As a result, the response on flat-top control voltage is saw-tooth current oscillating around the prescribed value with frequency of 10 kHz and amplitude of ±14 A.

The similar amplifier with 24 V battery bank controls the current in the radial field coils (20 mΩ, 70 μH).

4. REGULATION

As a first step, magnetic field at the beginning of the discharge must be properly chosen to perform favourable breakdown and current rise. Therefore, the currents in the servo-systems are externally preprogrammed before the discharge by external signals U_{ext} (fig. 1).

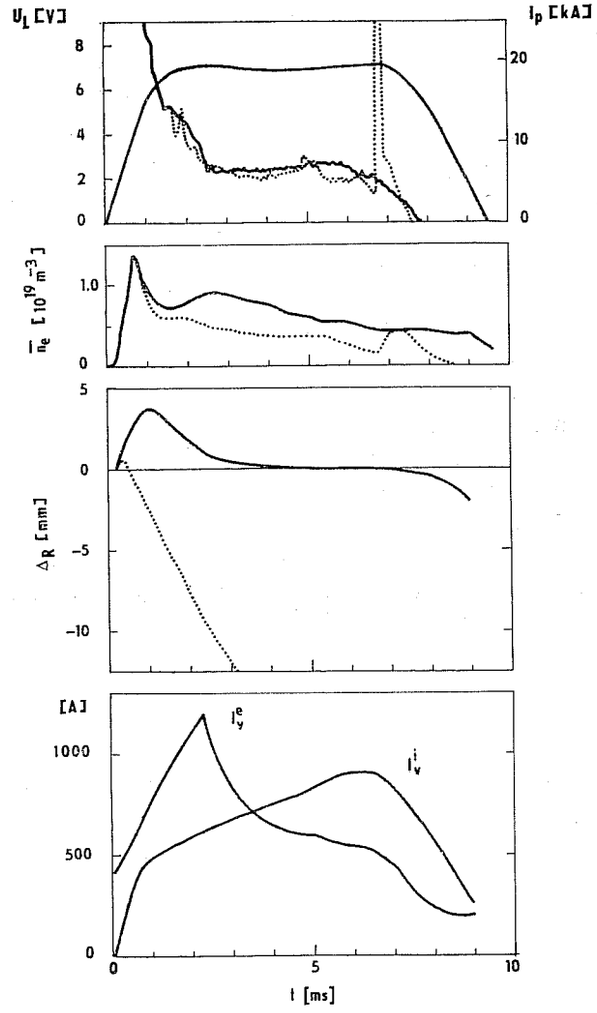

Fig. 2. Discharge with regulated radial plasma position (full lines) and discharge with scenario of poloidal magnetic fields previously used (dashed lines). U_L — loop voltage, I_p — plasma current (the same with and without regulation), $\bar{n}_e$ — line averaged electron density, Δ_R — radial plasma displacement. I^e_v — current in the external quadrupole coils (regulated by servo-system), I^i_v — current in the internal quadrupole coils (proportional to the primary transformer current). Both current waveforms I^e_v and I^i_v refer to the discharge with regulation.

a) Radial position

Since the power amplifier is unipolar it is necessary to adjust the current in the internal quadrupole system I^i_v so that $\Delta_R > 0$ for $G = 0$ during the whole disacharge. To obtain such current we remain the previous scheme in which this coil system is connected in series with the primary transformer coil but we add a shunt parallel

to the coils. Thus the amplitude of the current can be changed. Optimum is found if I_v^i is 45% of the primary transformer current. Its waveform is shown in fig. 2.

The regulation setting is adjusted empirically. For proportional regulation plasma displacement is always positive; pure integral regulation leads to oscillations with a period of about 10 ms. Minimal deviation is obtained as a compromise, by choosing $G = 9$ and $T_I = 2{\cdot}9$ ms. Figure 2 shows the discharge with regulated radial plasma position. It is seen that radial plasma displacement Δ_R is nearly zero except in the phases when plasma current changes. This is, however, a well-known effect that the stabilization of the plasma position during the current ramp-up and ramp-down phases is very difficult. Figure 2 shows the current in the external quadrupole coils I_v^e which is controlled by the servo-system. It starts from a preprogrammed non-zero level which is optimal for breakdown. During the plasma current ramp-up, I_v^e rises with saturated rate. Then it starts to be controlled by the servo-system in such a way that it continuously decreases nearly to zero at the end of the discharge. This is due to the increasing vertical magnetic field of internal coils and indicates that for longer pulses new waveform for I_v^i must be chosen.

In fig. 2, for comparison, a discharge with compensation scenario previously used is also shown. It is seen that the regulation improves plasma parameters, especially

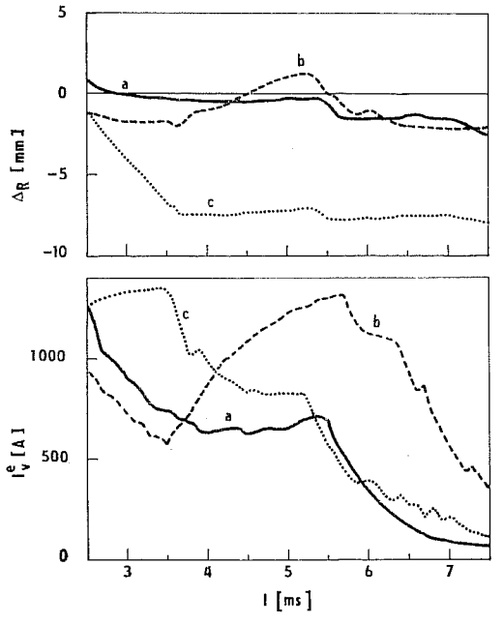

Fig. 3. Response of radial plasma position and servo-system on changes of plasma energy ($I_p = 12$ kA). a — discharge with kinetic instability at 5·5 ms; b — discharge with auxiliary injection of lower hybrid wave during 3·5 ÷ 5·5 ms; c — discharge with prescribed displacement at $\Delta_R = -8$ mm.

it removes positional disruption at the end of the discharge (positive spike on the loop voltage U_L). Thus the pulse durations is potentially prolonged.

The optimal regulation setting can be compared with result of stability analysis of the servo-loop (see e.g. [5]). Our situation, however, is complicated by a presence of the copper shell and a short duration of the discharge. Here, we restrict ourselves only to the decomposition of the equilibrium field and to the discussion of the system response on changes of plasma energy.

The vertical field needed for equilibrium is

$$B^{eq} = \frac{\mu_0 I_p}{4\pi R_0}\left(\ln\frac{8R_0}{a} - \tfrac{3}{2} + \beta_p + \tfrac{1}{2}l_i\right) = 13{\cdot}3 \div 14{\cdot}8\ \mathrm{mT}\,,$$

for $I_p = 19$ kA and Shafranov factor $\Lambda = \beta_p + l_i/2 = 0{\cdot}7 \div 1{\cdot}0$. If $B_0^{e,i}$ are vertical magnetic fields of external and internal windings without the shell, then the actual fields in the chamber are given by the operator:

$$B^{e,i} = \hat{g}^{e,i}\, B_0^{e,i}(t) = h^{e,i}\, B_0^{e,i}(t) + (1 - h^{e,i}) \int_{-\infty}^{t} g^{e,i}(t' - t)\, B_0^{e,i}(t')\, \mathrm{d}t'\,.$$

The response of $\bar{B}_z$ on step-like currents $I_v^{e,i}$ shows that for $t = 0 \div 7$ ms, $h^{e,i} \approx 0{\cdot}24$, $0{\cdot}27$ and $g^{e,i}(t) \approx (1/\tau^{e,i}) \exp(-t/\tau^{e,i})$ with $\tau^{e,i} \approx 1{\cdot}26$ ms respectively. Then the field generated by coils (at $t = 6$ ms in fig. 2) equals

$$\hat{g}^e\, B_0^e(t) + \hat{g}^i\, B_0^i(t) \approx 1{\cdot}3\ \mathrm{mT} + 2{\cdot}2\ \mathrm{mT} = 3{\cdot}5\ \mathrm{mT}\,.$$

Thus the servo-system controls about 10% of the total equilibrium field.

At the same instant, the image field of the iron core can be estimated as

$$\gamma\, \hat{g}^e \left[\frac{\mu_0 I_p}{2\pi R_0}\, f(R_0/R_i)\right] \approx 4{\cdot}3\ \mathrm{mT}\,.$$

The expression under operator is the image field of an infinitely long cylinder with permeability $\mu = \infty$. The geometrical factor $f(R_0/R_i) = 1{\cdot}2$ [2]. The factor $\gamma = 0{\cdot}74$ includes a counter force of the external limbs.

The remaining fields $5{\cdot}5 \div 7{\cdot}0$ mT, is generated by those currents in the shell which are driven by poloidal field of the plasma. This value is consistent with the fact that the dynamics of these currents is governed approximately by $\hat{g}^i$ which acts on 6 ms pulses as $\hat{g}^i \approx 0{\cdot}5$.

The response of the servo-system on a change of internal plasma energy is illustrated in fig. 3. Sudden decrease is represented by a kinetic instability (fig. 3a). Since its time constant (≈ 100 μs) is shorter than diffusion time $t_d = \frac{1}{4}\mu_0\sigma d^2 = 1{\cdot}8$ ms the shell acts as a thick casing (σ is copper conductivity). Therefore the shift of plasma position is

$$\delta\Delta_R = \tfrac{1}{2}\left(1 - \frac{a^2}{b_s^2}\right)\frac{b_s^2}{R_0}\,\delta\Lambda - 2\pi\,\frac{b_s^2}{\mu_0 I_p}\,\delta B^e\,, \tag{2}$$

where δ denotes the changes during the instability. For observed shift and $\delta I_v^e \approx \approx -100$ A we obtain $\delta\Lambda = -0{\cdot}22$ and balance (2) reads as $\Delta_R = -1{\cdot}4$ mm + + 0·4 mm = −1 mm.

Slower increase of Λ is represented by an additional injection of RF energy into the plasma (fig. 3b). Here, we are just in the hybrid regime; neither thick nor thin shell approximation is valid. The servo-system is nearly saturated ($\delta B_0^e \approx 2{\cdot}4$ mT and $\hat{g}^e\,\delta B_0^e \approx 0{\cdot}9$ mT) and plasma shift is $\delta\Delta_R = +3$ mm.

Figure 3c illustrates the possibility of maintaining the plasma in the arbitrary prescribed position. It is made by a proper weighting of the plasma current signal in electronics, what correspondes to the change of the coefficient A_3 in eq. (1).

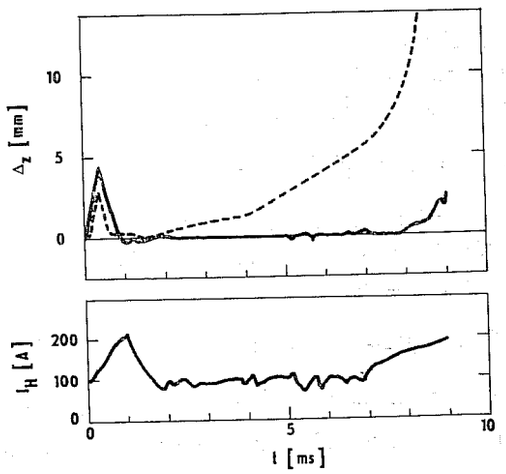

Fig. 4. Effect of regulation on vertical plasma position ($I_p = 19$ kA). Δ_z — vertical plasma displacement with (solid line) and without (dashed line) regulation, I_H — current in the horizontal magnetic field winding when regulation is applied.

b) Vertical position

Regulation of vertical position is demonstrated in fig. 4. The gain is set to $G = 10$ and $T_I = 5{\cdot}5$ ms. The value of horizontal magnetic field generated by servo-system corresponds to the horizontal components of stray field of the iron core. It is caused by the air gap under the upper horizontal limb. The position of the gap also ensures unipolarity of this filed.

5. CONCLUSION

The simple servo-system improves the plasma position on the CASTOR tokamak. A radial shift less than 3 mm is observed for common changes of the plasma energy. This value is approximately equal to the uncertainty in determining the plasma position. It arises from the following effects: (a) Detection coils are mounted with

an accuracy of 1 mm. (b) Internal quadrupole coils are placed very close to the plasma and thus magnetic boundary is elliptical. The difference between the axes can be estimated as [2]:

$$\frac{2\hat{g}^i I_v^i}{I_p} \cdot \frac{a^3}{b_s^2} \approx 2\text{ mm}$$

(for the shot in fig. 2). (c) Inhomogeneity of vertical magnetic field along the torus, typically $\delta B_z \approx 2$ mT, modulates the vertical plasma position with an amplitude of

$$\delta z \approx \frac{2\pi R_0}{6} \cdot \frac{\delta B_z}{B_T} \approx 1\text{ mm}\,.$$

The remaining contributions are small: offsets and uncompensated toroidal field leads to 0·1 V error on the position signal which for $I_p = 20$ kA gives 0·2 mm error in position. The relative error from calibration accuracy of coils, resistors and capacitors is 5%.

For comparison with other machines, the accuracy with which the plasma position is controlled has to be normalized to the minor radius; in our case it is 3·5%. For a servo-system in the TFTR tokamak, this relative accuracy is 2·5% [6].

The servo-system will allow us to prolong the discharge. For longer pulses, however, the current in the internal quadrupole coil system must be decoupled from the primary current.

The author thanks to Mr. J. Zelenka who performed a great deal of mechanical and cable-laying work. Dr. F. Žáček is gratefully acknowledged for his support.

Received 30 September 1988

References

[1] Valovič M.: Czech. J. Phys. B *38* (1988) 65.
[2] Mukhovatov V. S., Shafranov V. D.: Nuclear Fusion *11* (1971) 605.
[3] Dostál J.: Operational Amplifiers. Elsevier, Amsterdam, 1981.
[4] Schenk G.: MVA Amplifier used for Plasma Position Control in the WEGA Tokamak. Report EUR-CEA-FC-1140, February 1982.
[5] Hugill J., Gibson A.: Nuclear Fusion *14* (1974) 611.
[6] Coonrod J., Bell M. G., Hawryluk R. J., Mueller D., Tait G. D.: Rev. Sci. Instrum. *56* (1985) 941.